PCCP
INVITED ARTICLE

Excited-state hydrogen detachment and hydrogen transfer driven by repulsive $^1\pi\sigma^*$ states: A new paradigm for nonradiative decay in aromatic biomolecules

A. L. Sobolewski,[a] W. Domcke,*[b] C. Dedonder-Lardeux[c] and C. Jouvet[c]

[a] *Institute of Physics, Polish Academy of Sciences, PL-02668, Warsaw, Poland. E-mail: sobola@ifpan.edu.pl*
[b] *Institute of Physical and Theoretical Chemistry, Technical University of Munich, D-85747, Garching, Germany. E-mail: domcke@ch.tum.de*
[c] *Laboratoire de Photophysique Moleculaire du CNRS, Universite Paris-Sud, Bât. 210, F-91405, Orsay Cedex, France. E-mail: christophe.jouvet@ppm.u-psud.fr*

Received 29th November 2001, Accepted 31st January 2002
First published as an Advance Article on the web

The combined results of *ab initio* electronic-structure calculations and spectroscopic investigations of jet-cooled molecules and clusters provide strong evidence of a surprisingly simple and general mechanistic picture of the nonradiative decay of biomolecules such as nucleic bases and aromatic amino acids. The key role in this picture is played by excited singlet states of πσ* character, which have repulsive potential-energy functions with respect to the stretching of OH or NH bonds. The $^1\pi\sigma^*$ potential-energy functions intersect not only the bound potential-energy functions of the $^1\pi\pi^*$ excited states, but also that of the electronic ground state. *Via* predissociation of the $^1\pi\pi^*$ states and a conical intersection with the ground state, the $^1\pi\sigma^*$ states trigger an ultrafast internal-conversion process, which is essential for the photostability of biomolecules. In protic solvents, the $^1\pi\sigma^*$ states promote a hydrogen-transfer process from the chromophore to the solvent. Calculations for chromophore–water clusters have shown that a spontaneous charge-separation process takes place in the solvent shell, yielding a microsolvated hydronium cation and a microsolvated electron. These results suggest that the basic mechanisms of the complex photochemistry of biomolecules in liquid water can be revealed by experimental and theoretical investigations of relatively small chromophore–water clusters.

1. Introduction

The aromatic amino acids tryptophan and tyrosine and the nucleic acid bases adenine, guanine, cytosine and thymine represent some of the most important building blocks of life. A characteristic feature of the photochemistry of these molecules in the condensed phase is the extremely low quantum yield of fluorescence of the strongly UV absorbing singlet ππ* excited states, indicating the existence of very fast nonradiative processes which efficiently quench the fluorescence.[1,2] It is conceivable that the evolution of life has selected molecular building blocks with particularly short excited-state lifetimes to minimize dangerous photoreactions in living cells. The nonradiative processes presumably are ultrafast internal conversion (IC) back to the electronic ground state and photoionization (formation of solvated electrons) in aqueous solution.[3] They quickly dissipate the photon energy before more profound chemical rearrangements can take place. This so-called photostability is obviously particularly essential for the constituents of the DNA which encode the genetic information of all living matter.

It is also well known that the fluorescence lifetimes of tryptophan and its chromophore, indole, depend very sensitively on the environment.[4] This property can be used to obtain information on the dynamics of proteins.[5] The commonly accepted explanation of this behavior is the vibronic mixing and inversion of the lowest two $^1\pi\pi^*$ states of indole in polar environments.[2,4] These states are commonly labeled as L_a and L_b, following a suggestion of Platt for the classification of states in alternate hydrocarbons. The L_a–L_b interconversion invoked to explain the quenching of fluorescence in indole and tryptophan[6] does not convincingly explain, however, the ultrashort lifetime of the fluorescing state. In fact, it has been argued that vibronic interaction with a third, so far unknown, electronic state is necessary to explain the observations in indole and 3-methylindole.[7]

In recent years, the spectroscopy of isolated biomolecules as well as size-selected clusters of biomolecules with typical solvent molecules has provided a significant amount of new and precise information on these systems. The spectroscopy and photochemistry of clusters of indole and phenol (the chromophore of tyrosine) with water and ammonia, for example, have been investigated in great detail, see refs. 6 and 8–12 and references therein. The isolated DNA bases, their clusters with water, and nucleic-acid base pairs have recently been investigated with laser-induced fluorescence (LIF) and resonance-enhanced multi-photon (REMPI) spectroscopy.[13–17] While the pyrimidine bases uracil and thymine exhibit only broad and diffuse REMPI spectra and lack fluorescence even under isolated-molecule conditions,[13] [13], the purine bases adenine and guanine show sharp REMPI and LIF spectra, albeit only in a very narrow energy range.[14–16] In all DNA bases a low-lying nonradiative threshold is observed, at which an abrupt quenching of the fluorescence occurs.[14–16] It has been suggested that $^1\pi\pi^*$–$^1n\pi^*$ coupling is responsible for the fluorescence quenching of the $^1\pi\pi^*$ state of the DNA bases, but this argument does not provide an explanation of the postulated ultrashort lifetime of the $^1n\pi^*$ states.[14,15,18]

In this article, we collect evidence obtained in recent theoretical and experimental investigations for the existence of a simple and universal mechanism of ultrafast radiationless decay in aromatic biomolecules, namely hydrogen-detachment driven IC in the isolated systems and chromophore-to-solvent hydrogen transfer in clusters. The most complete set of data, both experimental and theoretical, is presently available for phenol and indole and their clusters with water and ammonia. The following discussion therefore will largely rely on these results. We shall also discuss preliminary theoretical results for adenine in comparison with experimental data. We propose that our findings for these representative systems are generic to all aromatic molecules containing hydroxy (OH) or azine (NH) groups.

2. Photochemistry of phenol, pyrrole and indole

The relevant potential-energy (PE) functions of phenol, indole and pyrrole are displayed in Fig. 1. For clarity, only the lowest $^1\pi\pi^*$ and $^1\pi\sigma^*$ states are shown. $^1n\pi^*$ states are located at higher energy in these systems and are not likely to be involved in the photochemistry of the lowest $^1\pi\pi^*$ states.

The curves shown are minimum-energy reaction-path profiles, that is, the values of all other coordinates have been optimized for a given value of the reaction coordinate. The reaction coordinate is the OH stretch coordinate of phenol and the NH stretch coordinate of pyrrole and indole, respectively. The geometries of the $^1\pi\pi^*$ and $^1\pi\sigma^*$ states have been optimized, while the ground-state energy is calculated at the $^1\pi\sigma^*$ optimized geometries. The geometry optimizations have been performed at the CASSCF level; single-point energy calculations along the reaction path have been performed with the CASPT2 method.[19] For more details, we refer to refs. 20–22.

The lowest $^1\pi\sigma^*$ state in these systems has previously been classified as a 3s Rydberg state.[23–25] An analysis of the wave function at the equilibrium geometry of the ground state indeed reveals the diffuse character of the σ^* orbital.[20–22] However, the stretching of the OH bond of phenol or the NH bond of pyrrole/indole leads to a collapse of the antibonding σ^* orbital towards the 1s orbital of hydrogen. This Rydberg-to-valence orbital transformation is reflected by the double-well shape of the $^1\pi\sigma^*$ PE function in pyrrole and indole, see Fig. 1(b)and (c). A shallow barrier separates the inner Rydberg part of the PE function from the outer valence part, which is repulsive. Interestingly, the repulsive $^1\pi\sigma^*$ PE function intersects not only the $^1\pi\pi^*$ PE functions (in phenol and indole), but also the ground-state PE function. These symmetry-allowed intersections of $^1A'$ and $^1A''$ states are converted into conical intersections when out-of-plane modes are taken into account.[26]

The generic shape of the $^1\pi\sigma^*$ PE function in these systems derives from two simple properties of the electronic structure. First, the σ^* natural CASSCF orbital is, as shown in Fig. 2 for phenol, indole and pyrrole, localized on the OH or NH bond, respectively, and is antibonding with respect to this bond. This localization and the antibonding character provide a strong driving force for the detachment of the H atom in the $^1\pi\sigma^*$ state. Second, the intersection of the $\pi\sigma^*$ state of $^1A''$ symmetry with the ground state of $^1A'$ symmetry is enforced by symmetry in planar systems. The $^1\pi\sigma^*$ state correlates asymptotically with the $^2\pi$ ground state of the phenoxyl, indolyl or pyrrolyl radical and the hydrogen atom in the 1s state, which is the lowest dissociation limit. Being of $^1A'$ symmetry, the ground state cannot correlate with this lowest dissociation limit of $^1A''$ symmetry. The $^1A'$ ground state thus must correlate to a higher dissociation limit, corresponding to a $^2\sigma$ excited state of the radical. The existence of a conical intersection of the lowest $^1\pi\sigma^*$ state with the ground state is thus a generic property of planar aromatic systems for which the ground state of the hydrogen-abstracted radical is of $^2\pi$ character. This simple relationship between the energetic ordering of the π and σ structures of aromatic radicals and potential-energy crossings of the corresponding closed-shell systems has been inferred long ago by Evleth and collaborators on the basis of semiempirical molecular-orbital calculations.[27,28]

The key point for the photophysics is the predissociation of the optically excited $^1\pi\pi^*$ state by the repulsive and optically dark $^1\pi\sigma^*$ state. The different photophysical dynamics of these systems can be understood in terms of the relative location of the $^1\pi\sigma^*$ and the $^1\pi\pi^*$ states. When the $^1\pi\sigma^*$ surface is below the $^1\pi\pi^*$ surface over most of the relevant nuclear configuration space, as in pyrrole (*cf.* Fig. 1(c)), there is fast internal conversion from the $^1\pi\pi^*$ to the $^1\pi\sigma^*$ state, and the photochemistry is determined by the dynamics of the $^1\pi\sigma^*$ surface and its conical intersection with the ground state. The conical intersection may cause ultrafast IC to the ground state, or alternatively, may lead to H atom detachment. This explains the complete absence of fluorescence in pyrrole. A weak fluorescence and weak and diffuse absorption lines assigned to the $^1\pi\sigma^*$ state have been observed, on the other hand, in *N*-methyl

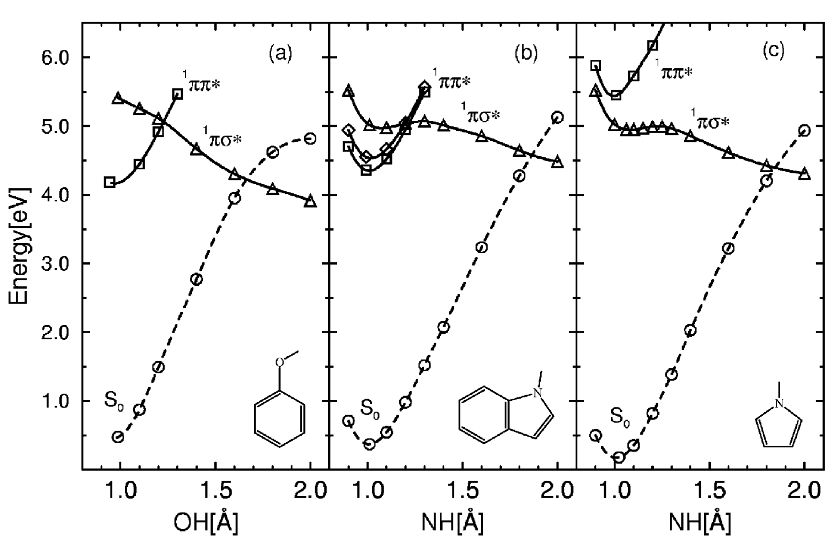

Fig. 1 PE profiles of the lowest $^1\pi\pi^*$ states (squares and diamonds), the lowest $^1\pi\sigma^*$ state (triangles) and the electronic ground state (circles) as a function of the OH stretch (phenol) or NH stretch (indole, pyrrole) reaction coordinate. Geometries have been optimized in the excited electronic states at the CASSCF level; the PE profiles have been obtained with the CASPT2 method.

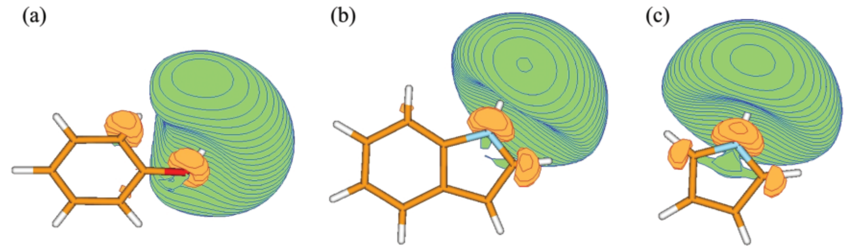

Fig. 2 The σ^* natural orbital obtained by a CASSCF calculation for the $^1\pi\sigma^*$ state of (a) phenol, (b) indole, and (c) pyrrole at the ground-state equilibrium geometry.

pyrrole,[29] which is understandable in the light of the above discussion.

When the minimum of the $^1\pi\pi^*$ surface is lower than the minimum of the flat $^1\pi\sigma^*$ surface, like in phenol and indole, a $^1\pi\pi^*$–$^1\pi\sigma^*$ curve crossing occurs at intermediate OH/NH distances (*cf.* Fig. 1(a) and (b)). The photochemical dynamics is then crucially dependent on the energetic location of the crossing and the excess energy available in the $^1\pi\pi^*$ state. Excitation below the minimum of the $^1\pi\pi^*$–$^1\pi\sigma^*$ crossing seam results in sharp spectra and a high quantum yield of fluorescence. Excitation above the crossing seam, on the other hand, results in diffuse absorption spectra and a complete quenching of the fluorescence.

The qualitative topography of the adiabatic PE surfaces resulting from the crossing of a repulsive $^1\pi\sigma^*$ state with bound $^1\pi\pi^*$ and S_0 states is illustrated in Fig. 3. The S_1 surface typically exhibits a local minimum of $^1\pi\pi^*$ character in the vicinity of the equilibrium geometry of the ground state. The upper ($^1\pi\pi^*$–$^1\pi\sigma^*$) conical intersection typically induces a barrier on the S_1 surface, which separates the local $^1\pi\pi^*$ minimum from the conical intersection of $^1\pi\sigma^*$ with S_0 (*cf.* Fig. 3). This barrier is likely to be responsible for pronounced isotope effects on the fluorescence lifetime and quantum yield. It should be kept in mind that Fig. 3 is an oversimplification of the actual situation, since the coupling modes are in general different for the $^1\pi\pi^*$–$^1\pi\sigma^*$ and $^1\pi\sigma^*$–S_0 conical intersections.[26]

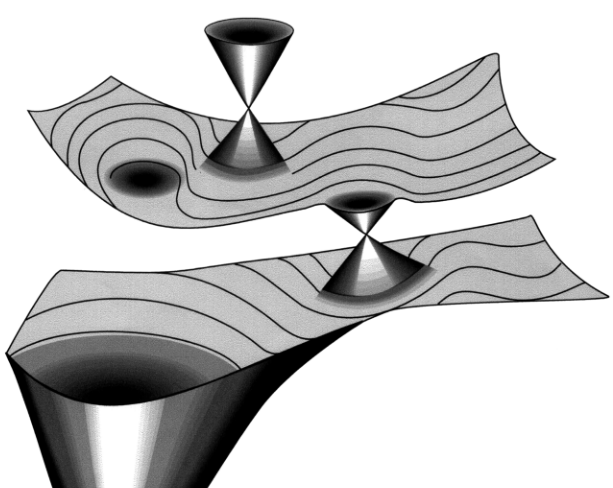

Fig. 3 Schematic view of the conically intersecting S_0, $^1\pi\pi^*$, and $^1\pi\sigma^*$ PE surfaces. The upper (lower) cone arises from the intersection of the repulsive $^1\pi\sigma^*$ surface with the $^1\pi\pi^*$ (S_0) surface.

The PE functions shown in Fig. 1 and 3 provide us with a qualitative explanation of the photophysical behavior of phenol, indole and related chromophores. The fluorescence lifetime of the vibrationless level of the $^1\pi\pi^*$ state of phenol is 2 ns, whereas the corresponding lifetime for the deuterated phenol (C_6H_5OD) is 16 ns,[30–32] which indicates that the lifetime is controlled by a tunneling process. The existence of a low barrier towards hydrogen detachment also explains why the fundamental of the OH stretch vibration could not be observed in the S_1 state:[33] the $v = 1$ level of the OH vibration dissociates too quickly. The very short lifetime of the $S_2(\pi\pi^*)$ state of phenol (shorter than 350 fs[34]) can be understood either in terms of $S_2 - S_1$ IC, yielding the S_1 state with an excess energy which is larger than the barrier towards dissociation, or a direct crossing of $S_2(\pi\pi^*)$ with the repulsive $^1\pi\sigma^*$ state.

The energy of the $S_1(\pi\pi^*)$ excited state relative to the repulsive $^1\pi\sigma^*$ state also is a governing factor of the photophysical behavior. If the S1($\pi\pi^*$) state is low in energy as in polycyclic aromatics (*e.g.*, naphthol *vs.* phenol), more excess energy in the S_1 state is required to reach the nonradiative threshold.

In indole derivatives, *e.g.* 3-methylindole and 2,3-dimethylindole, it has been found that the lifetime shortens as the excess energy increases in the $S_1(\pi\pi^*)$ state, while in the deuterated species the lifetime is longer and does not change much with excitation energy,[35] which again indicates control of the lifetime by a tunneling mechanism. The ^1L_a–^1L_b coupling alone cannot explain these observations.[17]

While the spectroscopic studies provide direct information on the barrier associated with the $^1\pi\pi^*$–$^1\pi\sigma^*$ conical intersection, they do not tell us much about the dynamics at the $^1\pi\sigma^*$–S_0 conical intersection. The dynamics depends not only on the dissociative motion of the H atom, but also on the character of the coupling mode (*i.e.*, the out-of-plane mode which couples the $^1A''(\pi\sigma^*)$ state with the S_0 state at the intersection) and the coupling strength. Information on this coupling has so far only been obtained for malonaldehyde, where it was found that the coupling mode consists of essentially pure out-of-plane motion of the dissociating H atom.[26,36] Involving mostly motion of the light hydrogen atom, this conical intersection should result in an extremely fast IC process. (For comparison, the IC timescale of the conical intersection of the two lowest energy surfaces of the H_3 molecule has been estimated experimentally and theoretically as 3–6 fs.[37,38]) Fig. 3 indicates that one should expect a branching of the chemical dynamics into repopulation of the S_0 state of the parent molecule and dissociation to ground-state radicals and H atoms. When the former process takes place, the photon energy is converted into heat, preserving the chemical identity of the molecule. This is presumably the dominant photochemical channel. H release of phenol after UV excitation in the energy range of the $S_2(\pi\pi^*)$ state has been observed, however, both in the condensed phase[39] and in the gas phase.[40] More detailed gas-phase investigations are necessary to establish that the H release is a direct process on the $^1\pi\sigma^*$ surface, rather than a statistical dissociation process on the ground-state surface. Very recently, H atom release has also been observed in free 2-hydroxypyridine for excitation wavelengths shorter than 243 nm.[41]

3. Photochemistry of indole in aprotic polar solvents

The electronic-structure information discussed in the preceding section also sheds new light on the origin of solvent effects on the spectroscopy of these systems. The pronounced sensitivity of the fluorescence behavior on the environment is a general property of biological chromophores.[1,2,4] The most comprehensive and detailed investigations have been performed for indole and tryptophan, see ref. 2 and references therein.

As mentioned above, the effect of a polar environment on the relative location of the L_a and L_b $^1\pi\pi^*$ states of indole and substituted indoles has been extensively discussed in the literature.[2,4,9,17,35] It has been argued that the L_a state, being more polar than the L_b state and the ground state, should be stabilized more than the L_b state by a polar or polarizable medium, and may thus move below the L_b state. This effect has been correlated with the drastic changes in the fluorescence properties of indole with increasing polarity of the medium.[42,43] Recent investigations on 3-methylindole and its complexes with various polar solvent molecules have revealed, however, that the dispersed L_a fluorescence is structured[44] and not broad and redshifted, as previously assumed.

The calculated dipole moments of the lowest electronic singlet states of indole in the ground-state equilibrium geometry are 1.87 (S_0), 1.55 (L_b), 6.12 (L_a) and 11.03 D ($^1\pi\sigma^*$),[20] see also ref. 45 and 46. The expected large dipole moment of L_a is thus confirmed by the calculations, but the dipole moment of the $^1\pi\sigma^*$ Rydberg-like state is, surprisingly, much higher. The explanation of the unexpectedly large dipole moment of the $^1\pi\sigma^*$ state of indole is provided by Fig. 2, which shows that the $\pi \rightarrow \sigma^*$ excitation involves the shift of the electronic charge from the aromatic ring to the hydrogen atom of the NH group.

While the closely spaced L_a and L_b states of indole are likely to invert in a polar medium,[42–44] a pronounced lowering of the repulsive $^1\pi\sigma^*$ state must also take place. As is schematically shown in Fig. 4, the barrier separating the $S_1(\pi\pi^*)$ minimum from the $^1\pi\sigma^*$–S_0 conical intersection can thus essentially be eliminated, resulting in a complete quenching of the fluorescence, as observed experimentally.[2,4] The variation of the lifetime of tryptophan with the protein structure can likewise be viewed as arising from the variation of the energy of the $^1\pi\pi^*$–$^1\pi\sigma^*$ crossing, depending on the local environment.

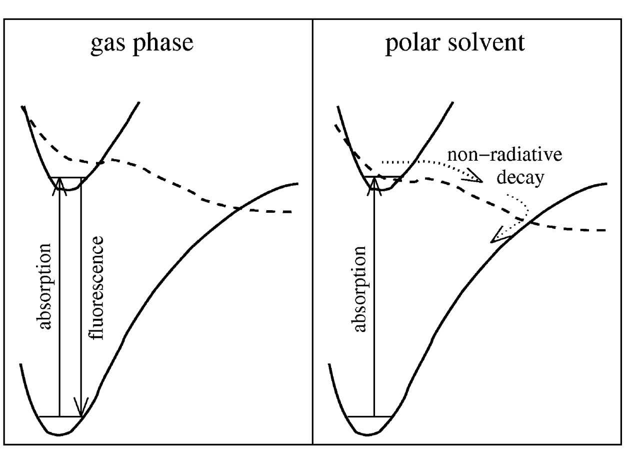

Fig. 4 Schematic illustration of the effect of a polar nonprotic environment on the photophysics of an aromatic chromophore, *e.g.* indole.

4. Photochemistry of clusters of phenol and indole with water and ammonia

If, as suggested above, hydrogen detachment is the primary photochemical process in biomolecular chromophores, then a substantial modification of the photochemistry is expected in hydrogen-accepting solvents. The size-specific spectroscopy of jet-cooled clusters of phenol/indole with water and ammonia is ideally suited to investigate this question. It is known that the reaction $H + H_2O \rightarrow H_3O$ is endothermic, while the reaction $H + NH_3 \rightarrow NH_4$ is approximately isothermic. Ammonia is thus a better hydrogen acceptor than water. We may thus expect characteristic differences between the photochemistry of phenol(indole)–water and phenol(indole)–ammonia clusters. Detection of the ammonium radical, in particular, can serve as a sensitive probe of photochemically induced hydrogen-detachment processes.[11,47–49]

Reaction paths and PE profiles for excited-state chromophore-to-solvent hydrogen transfer reactions have been obtained recently for clusters of phenol and indole with water and ammonia.[22,50,51] As representative examples, we discuss here the phenol–H_2O and phenol–NH_3 clusters.

The CASPT2 PE functions calculated along the minimum-energy reaction path for hydrogen atom transfer between phenol and water/ammonia are shown in Fig. 5. The corresponding PE functions for hydrogen detachment of free phenol have been given in Fig. 1(a). The most notable effect of the complexation of phenol with water or ammonia is the removal of the conical intersection of the $^1\pi\sigma^*$ state with the electronic ground state. In comparison with free phenol or phenol(indole) in aprotic solvents, the S_0 energy is lowered for large $O_{ph}H$ distances due to the stabilization of the ion-pair configuration in the ground-state wave function, *i.e.*, the ground-state proton-transfer species $PhO^-H_3O^+$ or $PhO^-NH_4^+$. The $^1\pi\sigma^*$ energy, on the other hand, is pushed upward at large $O_{ph}H$ distances, resulting in a shallow minimum of the $^1\pi\sigma^*$ surface. This minimum corresponds to a biradical configuration, consisting of a phenoxyl radical, $C_6H_5O^•$, and a hydronium, $H_3O^•$, or ammonium, $NH_4^•$, radical, respectively. An H atom has thus been transferred between phenol and the solvent molecule. In view of the nonfluorescent character of the $^1\pi\sigma^*$ state and the relatively large energy gap to the ground state, the hydrogen-transferred complex should be metastable as long as the O–O (O–N) distance is kept fixed. In fact, due to the strongly repulsive character of the $^1\pi\sigma^*$ state, the sol-

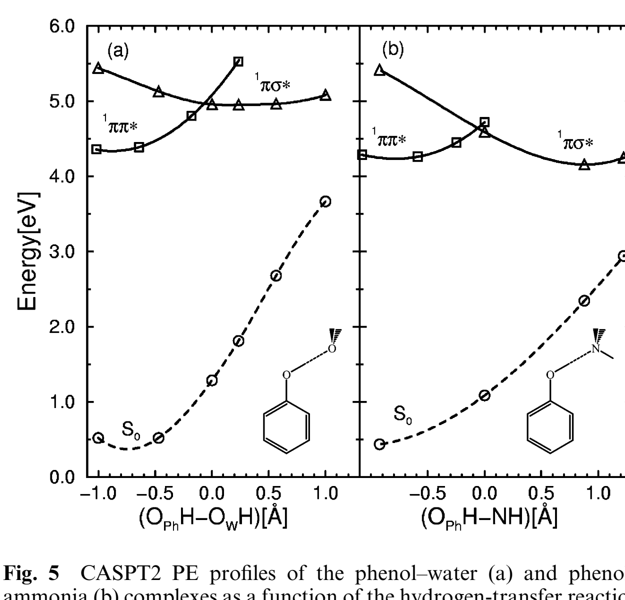

Fig. 5 CASPT2 PE profiles of the phenol–water (a) and phenol–ammonia (b) complexes as a function of the hydrogen-transfer reaction coordinate. Squares: $^1\pi\pi^*$ state; triangles: $^1\pi\sigma^*$ state; circles: S_0 state.

vated hydronium (ammonium) cluster may be ejected by the collision of the fast H atom with the solvent shell. The fast IC process to the electronic ground state, present in the bare molecule, is thus effectively quenched in the solvated phenol molecule.

More insight into the nature of the hydrogen-transfer process is provided by the electronic wave functions, in particular the σ* orbitals. Fig. 6 displays the σ* orbital of phenol–H_2O and phenol–NH_3, both at the equilibrium geometry of the ground state (upper panel) and the equilibrium geometry of the $^1\pi\sigma^*$ state (lower panel). It is clearly seen that the σ* orbital attaches to the water (ammonia) molecule already at the geometry of vertical excitation, that is, the electronic excitation involves a chromophore-to-solvent electron-transfer process. When the geometry of the complex relaxes to the $^1\pi\sigma^*$ minimum, the proton follows the electron, forming the hydronium (ammonium) radical. The phenoxy and hydronium (ammonium) radicals are connected by a strong hydrogen bond. The net hydrogen-transfer reaction is thus actually a concerted electron- and proton-transfer process.[22]

It is noteworthy that the energetics of the hydrogen-transfer process is different in phenol–water and phenol–ammonia.[22] As can be seen in Fig. 5, the H-transfer process is endothermic in phenol–H_2O, while it is exothermic in phenol–NH_3. The $^1\pi\pi^*$ and $^1\pi\sigma^*$ minima in phenol–NH_3 are separated by a barrier, however, which is located near the $^1\pi\pi^*$–$^1\pi\sigma^*$ PE crossing.

These computational results are helpful for the interpretation of the large amount of spectroscopic and kinetic data which have been collected in recent years for phenol–water and phenol–ammonia clusters.[6–8] Some of the observations are:

(i) The fluorescence lifetime of the $^1\pi\pi^*$ origin of the phenol–H_2O complex is of the order of 15 ns,[31] longer than in free phenol. This is in accord with the high energy of the crossing of the $^1\pi\pi^*$ and $^1\pi\sigma^*$ states and the endothermicity of the H-transfer reaction in the phenol–water cluster (*cf.* Fig. 5(a)). Indeed, no signature of H transfer has been observed in phenol–H_2O. In the phenol–NH_3 complex, on the other hand, the fluorescence lifetime of the 0–0 line is 1.2 ns, shorter than in free phenol, and the H-transfer reaction leading to the phenoxyl radical and NH_4 has recently been detected.[11,47,49] This is strong evidence that the $^1\pi\pi^*$ lifetime in phenol–ammonia complexes is determined by the excited-state hydrogen-transfer reaction.

(ii) The reaction rate for H-transfer depends strongly on the excess energy in the $S_1(\pi\pi^*)$ state in a mode-specific manner. The lifetime of the phenol–ammonia complex decreases when internal vibrations of phenol are excited: from 1.2 ns for the 0–0 transition to 370 ps for a ring vibration (786 cm^{-1}) of phenol, and to 390 ps, when the intermolecular O–H–NH_3 stretching coordinate with an energy of 182 cm^{-1} is excited.[52]

(iii) The $^1\pi\pi^*$ lifetime of phenol–$(NH_3)_n$ clusters decreases when the cluster size increases. In this case the H-transfer reaction is experimentally well characterized, since the solvated ammonium radicals, $NH_4(NH_3)_{n-1}$, which are formed by the dissociation of the hot clusters after the exothermic H transfer, are long-lived species (lifetimes in the (s range) which can be detected by ionization[52] or IR spectroscopy.[47] The $^1\pi\pi^*$ lifetime of the phenol$(NH_3)_2$ complex has been determined to be 400 ps, and it drops to 50 ps for the phenol$(NH_3)_3$ complex.[52] These findings are easily understood in terms of the lowering of the barrier associated with the $^1\pi\pi^*$–$^1\pi\sigma^*$ curve crossing upon solvation. Owing to its large dipole moment, the $^1\pi\sigma^*$ state is stabilized more than the $^1\pi\pi^*$ state, which leads to a decrease and eventually disappearance of the barrier.

An interesting by-product of the computational studies for phenol(indole)–$(H_2O)_n$ clusters is the discovery of a spontaneous charge-separation process within the $H_3O(H_2O)_{n-1}$ clusters.[22,50,51] The phenomenon is illustrated in Fig. 7 for the phenol$(H_2O)_3$ cluster. At the equilibrium geometry of the $^1\pi\sigma^*$ state, the structure consists of a phenoxyl radical, a H_3O^+ cation, and a localized electron cloud, which is solvated by two water molecules. The H_3O radical thus decomposes into a hydronium cation and a "solvated" electron, see Fig. 7. Calculations for neat $H_3O(H_2O)_{3m}$ clusters up to $m = 3$ have shown that this effect persists for larger clusters.[53] Moreover, the calculated electronic and vibrational spectra of these clusters show intriguing similarities with the spectra of the hydrated electron in liquid water.[54] Electron ejection, that is, the formation of hydrated electrons, has long been known to be an important channel in the UV photochemistry of tryptophan and tyrosine in aqueous solution.[55,56] The calculations strongly suggest that the primary photochemical process is H-atom ejection; the H atom then spontaneously decomposes in the aqueous environment to form solvated H_3O^+ cations and solvated electrons.[53,54] Since this biologically highly relevant solvation process occurs already in small chromophore($H_2O)_n$ clusters, it should be amenable to investigation with precise spectroscopic techniques. It should also be mentioned that the electronic spectra measured for $NH_4(NH_3)_n$ clusters[57] show fast convergence towards the spectrum of the solvated electron in ammonia.[58] This observation is confirmed by a recent computational study of the electronic spectra of $NH_4(NH_3)_n$ clusters.[59]

5. Photochemistry of DNA bases

Up to now only relatively few calculations of the excited states of DNA bases with *ab initio* methods have been reported. The presence of several heteroatoms with lone pairs results in the existence of a number of low-lying $^1n\pi^*$ and $^1\pi\sigma^*$ states in addition to the $^1\pi\pi^*$ states, resulting in a rather complex electronic spectrum. Moreover, the DNA bases possess several tautomers of comparable energy in the electronic ground state, which is the consequence of the mobility of some of the hydro-

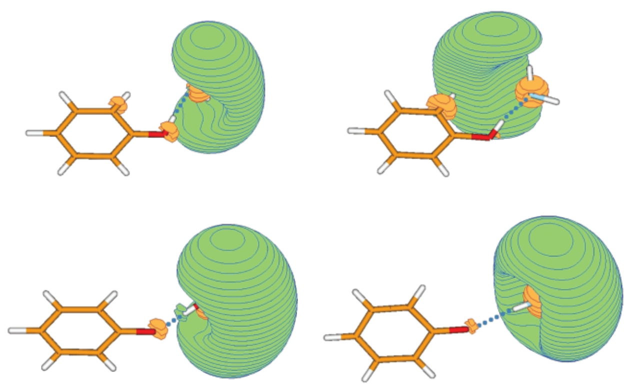

Fig. 6 The σ* natural orbital obtained by a CASSCF calculation for the $^1\pi\sigma^*$ state of the phenol–water complex (left) and the phenol–ammonia complex (right). Upper panel: wave function calculated at the ground-state equilibrium geometry; lower panel: wave function calculated at the $^1\pi\sigma^*$ equilibrium geometry.

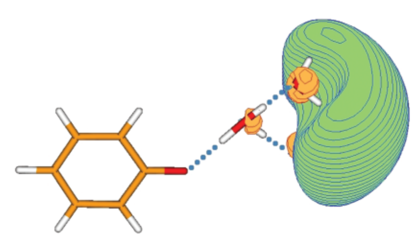

Fig. 7 The σ* orbital obtained by a CASSCF calculation for the $^1\pi\sigma^*$ state of phenol$(H_2O)_3$ at the $^1\pi\sigma^*$ equilibrium geometry.

gen atoms. Calculations of the vertical excitation spectra of adenine, guanine and cytosine by different methods have been reported in ref. 60–67. In a few cases, excited-state geometry optimizations have been performed for the lowest $^1\pi\pi^*$ and $^1n\pi^*$ states.[65–68]

Surprisingly, even the vertical excitation energies of the low-lying $^1\pi\sigma^*$ states in DNA bases seem to be unknown; at least these states have not been listed in the theoretical papers (with one exception, an early calculation on cytosine[60]), although it is clear that at least some of them must fall into the energy range of the lowest $^1\pi\pi^*$ states.

In a first exploratory study we have calculated the excited states and hydrogen-detachment reaction paths of adenine. The structure of the 9H tautomer of adenine is shown as an insert in Fig. 8. From the discussion in Sections 2 and 4 it is clear that this tautomer has two potentially active centers for hydrogen detachment, the azine (NH) group and the amino (NH_2) group. We thus expect two low-lying $^1\pi\sigma^*$ states, with the σ^* orbital localized on either of these groups. In addition, there must be low-lying $^1n\pi^*$ states, arising from the lone pairs of the nitrogen atoms. Since accurate CASSCF and CASPT2 calculations are tedious and time-consuming in this case of densely spaced excited states, the time-dependent density-functional-theory (TDDFT) method[69] with the B3LYP functional has been employed for the calculation of the reaction-path energy profiles. The reaction-path geometries of the excited states have been determined at the CASSCF level (the computational details are reported elsewhere[70]). To allow for a clear distinction of $\pi\pi^*$, $n\pi^*$ and $\pi\sigma^*$ states, the molecules have been constrained to the planar. (Geometry optimization of the ground state yields a slightly nonplanar amino group;[66] the energy lowering with respect to the planar form is of the order of a fraction of a kcal mol^{-1} and thus negligible for the present purposes.)

Fig. 8 shows PE profiles obtained as a function of the N_9H stretch coordinate of 9H-adenine. As before, the reaction paths have been optimized in the excited states, while the energy of the S_0 state is calculated at the $^1\pi\sigma^*$ optimized geometries. The TDDFT/B3LYP method cannot be expected to be sufficiently accurate to yield the correct ordering of the densely spaced excited states of adenine. Previous calculations have indicated, however, that the method may be reliable as far as the shape of hydrogen-transfer PE functions is concerned.[70]

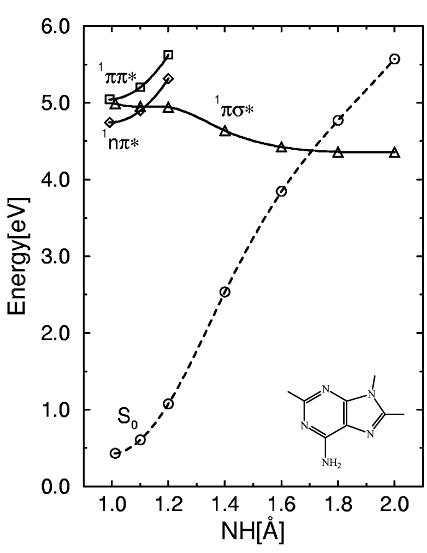

Fig. 8 PE profiles of the lowest $^1\pi\pi^*$ state (squares), the lowest $^1n\pi^*$ state (diamonds), the lowest $^1\pi\sigma^*$ state (triangles), and the S_0 state (circles) of 9H-adenine, as a function of the NH stretch reaction coordinate. Geometries have been optimized at the CASSCF level; the PE profiles have been obtained with the TDDFT method.

The photochemical behavior of the lowest $^1\pi\sigma^*$ state of 9H-adenine is seen to be exactly the same as found in phenol and indole (*cf.* Fig. 1). The $^1\pi\sigma^*$ PE profile exhibits the indication of a barrier which reflects the Rydberg-to-valence transformation of the σ^* orbital. Overall, the $^1\pi\sigma^*$ PE function is repulsive and exhibits symmetry-allowed crossings with the $^1\pi\pi^*$ and S_0 states. The lowest $^1n\pi^*$ state is bound like the $^1\pi\pi^*$ state with respect to hydrogen detachment. The crossing of the $^1\pi\sigma^*$ and $^1n\pi^*$ PE functions is, in principle, an avoided one, as both states are of $^1A''$ symmetry. The interaction of these two states appears to be weak, however.

Fig. 8 confirms that the conical intersection of the $^1\pi\sigma^*$ state with the S_0 state is a general phenomenon. Like in indole and phenol, the ground state dissociates towards an excited $^2\sigma$ radical, while the lowest $^1\pi\sigma^*$ state dissociates towards the $^2\pi$ ground state of the hydrogen-abstracted radical. The arguments outlined in sections 2–4 for indole and phenol and their clusters with water and ammonia thus apply analogously for adenine and, by implication, for the other DNA bases.

The particular role of a repulsive $^1\pi\sigma^*$ state has first been noted in calculations on the phototautomerization of 2-hydroxypyridine,[72] which can be considered as a simplified model of DNA bases. It has been shown that the phototautomerization of this system[73] likely involves a dissociation and re-attachment of the mobile hydrogen atom *via* a conical intersection with the ground state.[72]

The general picture of the photochemistry of isolated DNA bases is thus as follows. As a consequence of the reduced aromaticity of these molecules owing to the presence of several heteroatoms, the strongly absorbing $^1\pi\pi^*$ states are located relatively high in energy. This property narrows the energy gap between the threshold of absorption (the 0–0 line of the lowest $^1\pi\pi^*$ state) and the radiationless-decay threshold. The latter is determined by the minimum of the crossing seam of the $^1\pi\pi^*$ state with the lowest $^1\pi\sigma^*$ state. This qualitative picture (*cf.* the PE surfaces of Fig. 3) explains the rather short LIF spectra of jet-cooled purine bases, with sharp and isomer-specific cut-offs of the fluorescence. Since the $^1n\pi^*$ states are of the same symmetry species as the $^1\pi\sigma^*$ states for planar systems, they may interact more directly with the repulsive $^1\pi\sigma^*$ states and may therefore acquire shorter lifetimes. Indications of a shorter lifetime of $^1n\pi^*$ states have been found in several experiments.[14,15] In the condensed phase, the highly polar $^1\pi\sigma^*$ states are lowered relative to the less polar $^1\pi\pi^*$ and $^1n\pi^*$ states, resulting in a complete quenching of the fluorescence. Very short excited-state lifetimes have recently been determined for DNA nucleosides in aqueous solution.[74,75] In protic environments, the same hydrogen-transfer processes are expected as have been discussed above for phenol and indole. In clusters, this can lead to fast fragmentation (on a timescale of a few hundred femtoseconds), as recently observed for adenine–water clusters.[76]

6. Conclusions

We have pointed out in this article that excited electronic states of $^1\pi\sigma^*$ type play a pivotal role in the photochemistry of aromatic molecules, in particular those containing enol and azine groups. These $^1\pi\sigma^*$ states are dark in absorption (more precisely, they have very small transition dipole moments with the ground state) and their PE surfaces are dissociative along OH/NH stretch coordinates. These properties render their spectroscopic detection extremely difficult. Experimentally, the existence of these states can be inferred only indirectly, *via* the interpretation of the relaxation or fragmentation dynamics following photoexcitation. In this situation, *ab initio* computational chemistry provides an invaluable tool. The calculations have revealed the key features of these states, which are:

(i) $^1\pi\sigma^*$ PE functions are repulsive with respect to OH or NH stretch coordinates, and thus can predissociate the bound $^1\pi\pi^*$ and $^1n\pi^*$ states.

(ii) $^1\pi\sigma^*$ states are highly polar, which implies that their energetic location relative to the less polar $^1\pi\pi^*$ and $^1n\pi^*$ states is strongly dependent on the environment.

(iii) $^1\pi\sigma^*$ PE surfaces generically exhibit a conical intersection with the electronic ground-state PE surface; this intersection provides the mechanism for ultrafast internal conversion to the ground state.

The universally repulsive character of the $^1\pi\sigma^*$ states originates from three properties of the σ^* orbital: (a) it is completely localized on a single OH or NH group, (b) it is antibonding with respect to the OH or NH bond, and (c) upon stretching of the OH/NH bond, the 3s-type σ^* orbital collapses to the 1s orbital of the hydrogen atom, resulting in a large energy gain. The strongly polar character of $^1\pi\sigma^*$ states is a direct consequence of the localization of the σ^* orbital on the OH/NH bond: $\pi \rightarrow \sigma^*$ excitation shifts one electronic charge from the aromatic ring(s) towards the border of the molecule, resulting in a dipole moment of $\approx$10 D for typical enoles and heterocycles.[20–22] The generic conical intersection of the $^1\pi\sigma^*$ states with the ground state is a simple consequence of the fact that the ground state is of A' symmetry, and thus cannot correlate with the lowest dissociation limit, which corresponds to the aromatic π radical and the H(1s) atom and is of A'' symmetry in planar systems. The $^1A'$ ground state correlates asymptotically with a $^2\sigma$ excited state of the radical and must be intersected by the lowest $^1\pi\sigma^*$ state which correlates with the $^2\pi$ ground state of the radical.

It has also been shown in this article by reference to both experimental data and calculations that a hydrogen-accepting environment causes profound changes in the photochemical dynamics of aromatic chromophores. The presence of water or ammonia as solvent molecules removes the conical intersection of $^1\pi\sigma^*$ with S_0. Instead of IC to the electronic ground state, an excited-state hydrogen-transfer reaction takes place in clusters of phenol and indole with water or ammonia. Ammonia is a particularly good H-atom acceptor and thus can serve as a detector of the excited-state hydrogen-transfer reaction in clusters.[48,49] The calculations have shown, furthermore, that after hydrogen transfer from phenol or indole to water, a spontaneous charge separation process takes place, resulting in a hydronium cation and a localized solvated electron cloud.[22,50] This result reveals the microscopic mechanism of the production of solvated electrons in the UV photolysis of aromatic chromophores in liquid water.[55,56]

It has previously been pointed out in a theoretical investigation of the photochemistry of malonaldehyde that the photostability of typical excited-state intramolecular-proton-transfer systems such as *ortho*-hydroxybenzoxazoles or hydroxyphenylbenzotriazoles likely arises from ultrafast excited-state quenching *via* repulsive $^1\pi\sigma^*$ states and conical intersections with the ground state.[77] This conical intersection provides the mechanism for ultrafast return of the excited molecule to the electronic ground state, thus bypassing the potentially reactive triplet states. First experimental results with highest time resolution on the model system *o*-hydroxybenzaldehyde appear to support this picture.[78,79] It is intriguing that the mechanisms ensuring the photostability of the building blocks of life appear to be basically the same as those in commercial photostabilizers.

Acknowledgement

Financial support by the Deutsche Forschungsgemeinschaft and the Committee of Scientific Research of Poland (Grant No. 3 T09A 082 19) is gratefully acknowledged.

References

1 P.R. Callis, *Annu. Rev. Phys. Chem.*, 1983, **34**, 329.
2 D. Creed, *Photochem. Photobiol.*, 1984, **39**, 537.
3 A. Reuther, H. Iglev, R. Laenen and A. Laubereau, *Chem. Phys. Lett.*, 2000, **325**, 360.
4 P. R. Callis, *Methods Enzymol.*, 1997, **278**, 113.
5 P. Blandin, F. Merola, J. C. Brochon, O. Tremenau and A. Menez, *Biochemistry*, 1993, **33**, 2610.
6 J. W. Hager, D. R. Demmer and S. C. Wallace, *J. Phys. Chem.*, 1987, **91**, 1375.
7 D. R. Demmer, G. W. Leach and S. C. Wallace, *J. Phys.Chem.*, 1994, **98**, 12 834.
8 T. S. Zwier, *Annu. Rev. Phys. Chem.*, 1996, **47**, 205.
9 N. Mikami, *Bull. Chem. Soc. Jpn.*, 1995, **68**, 683.
10 K. Kleinermanns, M. Gerhards and M. Schmitt, *Ber. Bunsen-Ges. Phys. Chem.*, 1997, **101**, 1785.
11 Y. Huang and M. Sulkes, *J. Phys. Chem.*, 1996, **100**, 16 497.
12 G. Pino, G. Gregoire, C. Dedonder-Lardeux, C. Jouvet, S. Martenchard and D. Solgadi, *Phys. Chem. Chem. Phys.*, 2000, **2**, 893.
13 B. B. Brady, L. A. Peteanu and D. H. Levy, *Chem. Phys. Lett.*, 1988, **147**, 538.
14 N. J. Kim, G. Jeong, Y. S. Kim, J. Sung, S. K. Kim and Y. D. Park, *J. Chem. Phys.*, 2000, **113**, 10 051.
15 E. Nir, K. Kleinermanns, L. Grace and M. S. de Vries, *J. Phys. Chem. A*, 2001, **105**, 5106.
16 F. Piuzzi, M. Mons, I. Dimicoli, B. Tardivel and Q. Zhao, *Chem. Phys.*, 2001, **270**, 205.
17 E. Nir, K. Kleinermanns and M. S. de Vries, *Nature*, 2000, **408**, 949.
18 A. Broo, *J. Phys. Chem. A*, 1998, **102**, 526.
19 K. Andersson and B. O. Roos, in *Modern Electronic Structure Theory*, ed. D. R. Yarkony, World Scientific, Singapore, 1995, vol. 1, p. 55.
20 A. L. Sobolewski and D. Domcke, *Chem. Phys. Lett.*, 1999, **315**, 293.
21 A. L. Sobolewski and D. Domcke, *Chem. Phys. Lett.*, 2000, **321**, 479.
22 A. L. Sobolewski and D. Domcke, *J. Phys. Chem. A.*, 2001, **105**, 9275.
23 L. Serrano-Andres, M. Merchan, I. Nebot-Gil, B. O. Ross and M. Fülscher, *J. Am. Chem. Soc.*, 1993, **115**, 6184.
24 L. Serrano-Andres and B. O. Ross, *J. Am. Chem. Soc.*, 1996, **118**, 185.
25 J. Lorentzon, P.-A. Malmqvist, M. Fülscher and B. O. Ross, *Theor. Chim. Acta*, 1995, **91**, 91.
26 A. L. Sobolewski and D. Domcke, *Chem. Phys.*, 2000, **259**, 181.
27 E. M. Evleth, P. M. Horowitz and T. S. Lee, *J. Am. Chem. Soc.*, 1973, **95**, 7948.
28 E. M. Evleth, O. Chalvet and P. Balmiere, *J. Phys. Chem.*, 1977, **81**, 1913.
29 R. McDiarmid and X. Xing, *J. Chem. Phys.*, 1996, **105**, 867.
30 R. J. Lipert and S. D. Colson, *J. Phys. Chem.*, 1990, **94**, 2358.
31 R. J. Lipert, G. Bermudez and S. D. Colson, *J. Phys. Chem.*, 1988, **92**, 380.
32 R. J. Lipert and S. D. Colson, *J. Phys. Chem.*, 1989, **93**, 135.
33 T. Ebata, N. Mizuochi, T. Watanabe and N. Mikami, *J. Phys. Chem.*, 1995, **100**, 546.
34 C. P. Schick, S. D. Carpenter and P. M. Weber, *J. Phys. Chem.*, 1999, **103**, 10 470.
35 D. R. demmer, G. W. Leach, E. A. Outhouse, J. W. Hager and S. C. Wallace, *J. Phys. Chem.*, 1990, **94**, 582.
36 A. L. Sobolewski and W. Domcke, *J. Phys. Chem. A*, 1999, **103**, 4494.
37 R. Bruckmeier, C. Wunderlich and H. Figger, *Phys. Rev. Lett.*, 1994, **72**, 2550.
38 S. Mahapatra and H. Köpper, *Phys. Rev. Lett.*, 1998, **81**, 3116.
39 G. Köhler, G. Kittel and N. Getoff, *J. Photochem.*, 1982, **18**, 19.
40 C. Dedonder-Lardeux, D. Grosswasser, C. Jouvet and S. Martrenchard, to be published.
41 C. Jouvet *et al.*, to be published.
42 S. Arnold and M. Sulkes, *J. Phys. Chem.*, 1992, **96**, 4768.
43 M. J. Tubergen and D. H. Levy, *J. Phys. Chem.*, 1991, **95**, 2175.
44 K. W. Short and P. R. Callis, *J. Chem. Phys.*, 2000, **113**, 5235.
45 (*a*) P. R. Callis, *J. Chem. Phys.*, 1991, **95**, 4230; (*b*) P. R. Callis, *J. Phys. Chem.*, 1995, **99**, 8572.
46 L. Serrano-Andres and B.O. Roos, *J. Am. Chem. Soc.*, 1996, **118**, 185.
47 S. Ishiuchi, M. Saeki, M. Sakai and M. Fujii, *Chem. Phys. Lett.*, 2000, **322**, 27.

48 C. Dedonder-Lardeux, D. Grosswasser, C. Jouvet and S. Martrenchard, *Phys. Chem. Comm.*, 2001, **4**, 1.
49 G. Gregoire, C. Dedonder-Lardeux, C. Jouvet, S. Martrenchard and D. Solgadi, *J. Phys. Chem. A*, 2001, **105**, 5971.
50 A. L. Sobolewski and W. Domcke, *Chem. Phys. Lett.*, 2000, **329**, 130.
51 W. Domcke and A. L. Sobolewski, in *The Physics and Chemistry of Clusters*, ed. E. E. B. Campbell and M. Larsson, World Scientific, Singapore, 2001, p. 169.
52 G. Gregoire, C. Dedonder-Lardeux, C. Jouvet, S. Martrenchard, A. Peremans and D. Solgadi, *J. Phys. Chem. A*, 2000, **104**, 9087.
53 A. L. Sobolewski and W. Domcke, *J. Phys. Chem. A*, 2002in press.
54 A. L. Sobolewski and W. Domcke, *Phys. Chem. Chem. Phys.*, 2002, **4**, 4.
55 L. I. Grossweiner, G. W. Swenson and E. F. Zwicker, *Science*, 1963, **141**, 805.
56 D. V. Bent and E. Hayon, *J. Am. Chem. Soc.*, 1975, **97**, 2599.
57 S. Nonose, T. Taguchi, K. Mizuma and K. Fuke, *Eur. Phys. J. D*, 1999, **9**, 309.
58 T. R. Tuttle and S. Golden, *J. Phys. Chem.*, 1991, **95**, 5275.
59 K. Hashimoto, *Chem. Phys. Lett.*, 2001, **346**, 81.
60 H. J. A. Jensen, H. Koch, P. Jørgensen and J. Olsen, *Chem. Phys.*, 1988, **119**, 297.
61 J. M. O. Matos and B. O. Roos, *J. Am. Chem. Soc.*, 1988, **110**, 7664.
62 J. D. Petke, G. M. Maggiora and R. E. Christoffersen, *J. Am. Chem. Soc.*, 1990, **112**, 5452.
63 M. P. Fülscher, L. Serrano-Andres and B. O. Roos, *J. Am. Chem. Soc.*, 1997, **119**, 6168.
64 A. Broo and A. Holmen, *J. Phys. Chem.*, 1997, **101**, 3589.
65 A. Broo, *J. Phys. Chem. A*, 1998, **102**, 526.
66 B. Menucci, A. Toniolo and J. Tomasi, *J. Phys. Chem. A*, 2001, **105**, 4749.
67 B. Menucci, A. Toniolo and J. Tomasi, *J. Phys. Chem. A*, 2001, **105**, 7126.
68 E. L. Rachofsky, J. B. A. Ross, M. Krauss and O. Osman, *J. Phys. Chem. A*, 2001, **105**, 190.
69 E. K. U. Gross and W. Kohn, *Adv. Quant. Chem.*, 1990, **21**, 255.
70 A. L. Sobolewski and W. Domcke, to be published.
71 A. L. Sobolewski and W. Domcke, *Phys. Chem. Chem. Phys.*, 1999, **1**, 3065.
72 A. L. Sobolewski, *Chem. Phys. Lett.*, 1993, **211**, 293.
73 M. J. Novak, L. Lapinsky, J. Fulara, A. Les and L. Adamowicz, *J. Phys. Chem.*, 1992, **96**, 1562.
74 J. -M. L. Percourt, J. Peon and B. Kohler, *J. Am. Chem. Soc.*, 2001, **123**, 10 370.
75 J. Peon and A. H. Zewail, *Chem. Phys. Lett.*, 2001, **348**, 255.
76 N. J. Kim, H. Kang, G. Jeong, Y. S. Kim, K. T. Lee and S. K. Kim, *J. Phys. Chem. A*, 2000, **104**, 6552.
77 A. L. Sobolewski and W. Domcke, *Chem. Phys. Lett.*, 1999, **300**, 533.
78 S. Lochbrunner, T. Schultz, M. Schmitt, J. P. Schaffer, M. Z. Zgierski and A. Stolow, *J. Chem. Phys.*, 2002, **114**, 2519.
79 K. Stock, T. Bizjak and S. Lochbrunner, *Chem. Phys. Lett.*, 2002in press.